Dalton Transactions

PAPER

View Article Online
View Journal | View Issue



Cite this: *Dalton Trans.*, 2014, **43**, 7449

# Au nanoparticles on citrate-functionalized graphene nanosheets with a high peroxidase-like performance†

Xiaomei Chen,*[a,d] Xiaotian Tian,[a] Bingyuan Su,*[b] Zhiyong Huang,*[a] Xi Chen[c] and Munetaka Oyama[d]

In this paper, Au nanoparticles (AuNPs) have been homogeneously deposited on citrate-functionalized graphene nanosheets (Cit-GNs) by a simple one-pot reducing method. The morphology and composition of the thus-prepared AuNPs/Cit-GNs were characterized by transmission electron microscopy (TEM), high resolution TEM, energy dispersive X-ray spectroscopy and X-ray photoelectron spectroscopy. The results showed that the AuNPs with a uniform size are well dispersed on the surface of the Cit-GNs. Significantly, the as-prepared AuNPs/Cit-GNs possess intrinsic peroxidase-like activity, which can catalyze the oxidation of the peroxidase substrate 3,3,5,5-tetramethylbenzidine (TMB) by hydrogen peroxide ($H_2O_2$) to develop a blue color in aqueous solution. The catalysis was in accordance with Michaelis–Menten kinetics and the AuNPs/Cit-GNs showed a strong affinity for both $H_2O_2$ and TMB. Moreover, by comparing with Cit-AuNPs, AuNPs/GNs and AuNPs/PVP-GNs, the AuNPs/Cit-GNs composite exhibits a higher catalytic ability with a lower Michaelis constant ($K_m$) value, suggesting that the GNs with a large surface area and the citrate ions with more carboxyl groups around the AuNPs can greatly enhance the peroxidase-like activity of AuNPs/Cit-GNs. Taking the advantages of the high catalytic activity, the good stability and the low cost, the novel AuNPs/Cit-GNs represent a promising candidate as an enzyme mimic and may find a wide range of new applications in biochemistry and biotechnology.

Received 25th November 2013,
Accepted 17th January 2014

DOI: 10.1039/c3dt53316f

www.rsc.org/dalton

## Introduction

In recent years, considerable efforts have been expended on constructing enzyme mimics because natural enzymes bear some serious disadvantages, such as the sensitivity of their catalytic activity to environmental conditions, their low stability due to denaturation and the high costs in preparation and purification.[1,2] As hydrogen peroxide ($H_2O_2$) is an important oxidizing agent in biological systems, intense interest has grown in the development of the construction of efficient peroxidase mimics. By now, a large number of artificial mimics have been constructed by incorporating catalytic centers into various scaffolds to mimic natural peroxidase enzymes, such as hemin,[3] porphyrin,[4] DNAzyme,[5] molecularly imprinted hydrogels[6] and various nanoparticles (NPs).[7–20]

The rapidly emerging research fields of nanoscience and nanotechnology open new opportunities for the application of nanomaterials in catalysis. A series of nanostructured materials, such as magnetic nanomaterials ($Fe_3O_4$ NPs[7] and $Co_3O_4$ NPs[8]), carbon nanomaterials (helical carbon nanotubes,[9] carbon dots,[10] graphene oxide (GO)[11] and $C_{60}$-carboxyfullerenes[12]), noble metal NPs (AuNPs,[13–15] AgNPs[16] and PtNPs[17]) and other nanomaterials,[18–20] have been demonstrated to possess a peroxidase-like catalytic activity. Among these nanomaterials, AuNPs are especially attractive because of their easy preparation, excellent biocompatibility and optoelectronic properties.[21–23] Although Au is traditionally considered to be catalytically inert, its catalytic activity can be improved when stabilized on some metal oxide supports such as $TiO_2$,[24] $Fe_2O_3$,[25] ZnO,[26] or some capping agents.[13–15] Jv *et al.* reported that cysteamine-modified positively charged AuNPs can catalyze the oxidation of the peroxidase substrate 3,3,5,5-tetramethylbenzidine (TMB) by $H_2O_2$ to develop a blue color in aqueous solution.[13] However, they found that the positively charged AuNPs can easily aggregate, therefore, in their further

[a]*College of Biological Engineering, Jimei University, Xiamen, 361021, China. E-mail: xmchen@jmu.edu.cn*
[b]*Xiamen Center for Disease Control and Prevention, Xiamen, 361021, China. E-mail: bysu82@163.com*
[c]*State Key Laboratory of Marine Environmental Science, Xiamen University, Xiamen, 361005, China*
[d]*Department of Material Chemistry, Graduate School of Engineering, Kyoto University, Nishikyo-ku, Kyoto, 615-8520, Japan*
†Electronic supplementary information (ESI) available. See DOI: 10.1039/c3dt53316f

research, they use single-walled carbon nanotubes to disperse these positively-charged AuNPs.[14] In another research, Wang *et al.* pointed out that compared with the amino modified AuNPs, the negatively charged citrate-capped AuNPs can attract amino groups of TMB electrostatically, which exhibit a strong affinity with TMB as a reaction substrate.[15] These findings suggested that the modification of the AuNPs on a suitable support is of great importance to enhance their peroxidase-like catalytic activity.

Nowadays, graphene nanosheets (GNs) have become a sensational material due to their unique physical and chemical properties, such as an extremely high electric and thermal conductivity, a high strength and a large surface area.[27] These unique properties make GNs a promising candidate to disperse catalytically active metal NPs and a good support for heterogeneous catalytic processes.[28–30] In previous researches, AuNPs have been successfully dispersed on GNs by various methods. However, to the best of our knowledge, only few reports use these AuNPs/GNs composites as enzyme mimics,[31,32] and there are no reports concerning the function of the capping agents on the mimic behaviors of these AuNPs/GNs. Due to the large surface area of the GNs and the wide applications of the AuNPs in biosensors, it is of great interest to study the peroxidase-like catalytic activity of different capping agent modified AuNPs/GNs composites in the oxidation of peroxidase substrates.

In this paper, we described a simple and general approach to grow AuNPs on citrate-functionalized GNs (AuNPs/Cit-GNs) and studied their mimic behavior in the oxidation of TMB. It is surprising that the thus-prepared AuNPs/Cit-GNs possess intrinsic peroxidase-like catalytic activity. To elucidate the effect of the citrate and GNs, another three composites, AuNPs/GNs, AuNPs/PVP-GNs and Cit-AuNPs were prepared for a comparison study. Based on the results, the AuNPs/Cit-GNs showed a significantly higher catalytic activity in the oxidation of TMB with a stronger affinity for both $H_2O_2$ and TMB comparing with the AuNPs/GNs, AuNPs/PVP-GNs and Cit-AuNPs. Different from previous reports, this is the first study concerning the mimic behavior of the negative-charged AuNPs/Cit-GNs. This study should provide new insights into the utilization of this peroxidase-like activity of AuNPs/Cit-GNs in medical diagnostics and biotechnology.

# Experimental

### Materials

$H_2O_2$, ammonia solution, sodium citrate and ascorbic acid (AA) were purchased from Wako Pure Chemicals, Co. Ltd; graphite powder, $HAuCl_4$, TMB, 2,2-azino-bis(3-ethylbenzothiazoline-6-sulfonic acid) (ABTS), poly(*N*-vinyl-2-pyrrolidone) (PVP, K30, molecular weight = 30 000–40 000) and hydrazine were from Aldrich Chem Co. All other reagents were of analytical grade and used without further purification. The pure water for the solution preparation was from a Sartorius arium pro UV/DI system.

### Instrumentations

The morphologies and crystal structures of the products observed by transmission electron microscopy (TEM) and high-resolution TEM (HRTEM) using a TECNAI F-30 TEM with an acceleration voltage of 300 kV. Energy dispersive X-ray spectroscopy (EDX) analysis was used to identify the elemental composition of the complex. All TEM samples were prepared by depositing a drop of diluted suspension in water on a copper grid coated with carbon film. The electronic binding energies of the AuNPs/Cit-GNs were measured by X-ray photoelectron spectroscopy (XPS) analysis which was performed on a PHI Quantum 2000 Scanning ESCA Microprobe with a monochromatised microfocused Al X-ray source. All the binding energies were calibrated by C 1s as the reference energy (C 1s = 284.6 eV). The ultraviolet-visible (UV-vis) absorption spectra of the catalysts were measured on a UV 1240 V spectrometer (Shimadzu) and the time-dependent absorbance spectra were performed on a USB2000+ miniature fiber optic spectrometer (Ocean Optics).

### Preparation procedures

GO was prepared according to a modified Hummer's method.[33] 25 mg of the as-synthesized product was dispersed in 100 mL water to obtain a yellow-brown aqueous GO solution (0.25 mg $mL^{-1}$) with the aid of ultra-sonication. For the preparation of the Cit-GNs, 100 mg sodium citrate was added into 10 mL 0.25 mg $mL^{-1}$ GO dispersion, followed by stirring for 12 h. Then, 10 μL hydrazine solution (35 wt% in water) and 80 μL ammonia solution (25 wt% in water) were added. After being vigorously stirred for 5 min, the vial was put in an oil bath (95 °C) for 1 h. Finally, the stable black colloids (Cit-GNs) were centrifuged and dissolved in 10 mL water. For the preparation of PVP-GNs, 40 mg PVP was mixed with 10 mL 0.25 mg $mL^{-1}$ GO dispersion, followed by stirring for 12 h. The other procedures were the same with those of the Cit-GNs.

The Cit-AuNPs and surfactant-free AuNPs/GNs were prepared according to Ali Umar's[34] and Yin's[35] work, respectively. In a typical synthesis of AuNPs/Cit-GNs, 0.5 mL of the as-prepared Cit-GNs suspension, 0.05 mL of 10 mM $HAuCl_4$, 0.05 mL of 0.1 M NaOH and 0.05 mL of 0.1 M AA were mixed in a vial under vigorous stirring for 1 h at room temperature. Then, the product was centrifuged and washed to remove the remaining reagents. For the preparation of the AuNPs/PVP-GNs, PVP-GNs were used instead of Cit-GNs, and the other procedures were the same as those for the preparation of the AuNPs/Cit-GNs.

### Catalysis procedures

To investigate the peroxidase-like activity of these enzyme mimics, the catalytic oxidation of the peroxidase substrate TMB in the presence of $H_2O_2$ was measured. As the amount of enzyme mimic has a serious effect on the results, we strictly controlled the amount of Au in the catalytic reactions. In a standard procedure, 50 μL of 8 mM TMB, 20 μL of $H_2O_2$ (30%) and 20 μL of 0.05 mg $mL^{-1}$ of Au in enzyme mimics were

 

added into 2 mL sodium acetate buffer solution (pH = 3.8) at 40 °C. The reaction was carried out in a quartz cuvette with an optical path length of 1 cm and was monitored by observing the absorbance evolutions at 652 nm. The kinetic analysis was carried out by using 20 μL enzyme mimics (0.05 mg $mL^{-1}$ of Au) in a reaction volume of 2 mL sodium acetate buffer solution (pH = 3.8) with 200 μM TMB or 100 mM $H_2O_2$, unless otherwise stated. The Michaelis–Menten constant was calculated using the Lineweaver–Burk plot: $1/v_0 = (K_m/v_{max})(1/[S] + 1/K_m)$, where $v_0$ is the initial velocity, $v_{max}$ is the maximal reaction velocity, and [S] is the concentration of the substrate.

## Results and discussion

### The characterization of the AuNPs/Cit-GNs

A schematic illustration of the reaction mechanism for the synthesis of the enzyme mimics is shown in Scheme 1. The progress of the reaction was characterized by UV-vis spectroscopy. As shown in Fig. 1, the absorption peak of the GO dispersion was at 227 nm, and disappeared after the modification of citrate, indicating the conjugation of GO and citrate. Comparing with GO, the absorption peak of Cit-GNs red-shifts to 262 nm, and the absorptions in the whole spectral region are increased, indicating that the electronic conjugation within the GNs is restored upon the hydrazine reduction. After the reduction of $AuCl_4^-$, a new absorption peak appeared at 525 nm, which suggested the formation of the AuNPs. The inset shows that the color of the mixture changed from brown (Cit-GO) to black (Cit-GNs) and at last dark red (AuNPs/Cit-GNs) during the reaction, which is in agreement with the UV-vis absorption results.

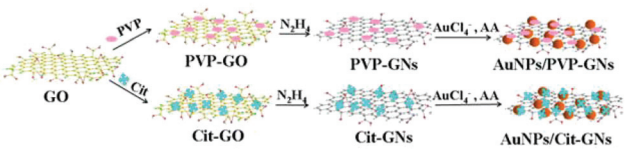


Scheme 1 A schematic illustration for the preparation of the AuNPs/Cit-GNs and AuNPs/PVP-GNs.

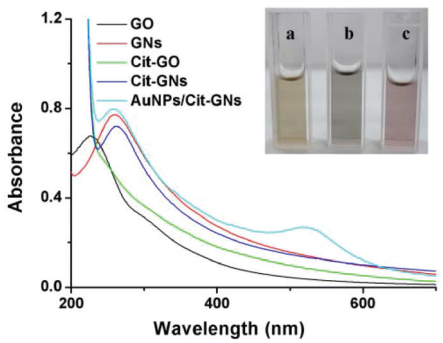


Fig. 1 The UV-vis absorption spectra of GO, GNs, Cit-GO, Cit-GNs and AuNPs/Cit-GNs. The inset shows the color of (a) Cit-GO, (b) Cit-GNs and (c) AuNPs/Cit-GNs.

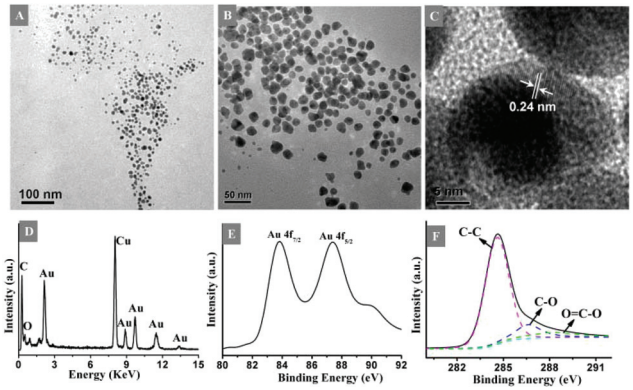


Fig. 2 (A and B) Representative TEM and (C) HRTEM images of the AuNPs/Cit-GNs. (D) The EDX spectrum of the AuNPs/Cit-GNs. (E and F) The XPS spectra of the Au 4f and C 1s of the AuNPs/Cit-GNs.

Fig. 2A–C show representative TEM images of the product at different magnifications. The low-magnification TEM image (Fig. 2A) shows that all of the AuNPs were uniformly dispersed on the surface of the GNs. The magnified image (Fig. 2B) reveals that the average size of these AuNPs was about 25 ± 2 nm. The HRTEM image (Fig. 2C) indicates that these AuNPs presented a single-crystalline structure. The inter-planar spacing is 0.24 nm, which agrees well with the (111) lattice spacing of the face-centered-cubic (fcc) Au. Fig. 2D shows a typical EDX analysis of the prepared AuNPs/Cit-GNs composite, in which an obvious Au peak could be found, suggesting that the AuNPs were successful prepared on the GNs surface. The formation of the AuNPs/Cit-GNs composite was further characterized by the XPS technique (Fig. 2E and F). It is clear that the resulting AuNPs/Cit-GNs show the doublet $4f_{7/2}$ and $4f_{5/2}$ peaks, which are corresponding to the metallic state of Au(0). Additionally, from the C 1s curves, only one peak associated with C–C can be observed, suggesting that the oxygenated functional groups (C–O, C═O) are substantially reduced by hydrazine. These results further supported the successful formation of the AuNPs/Cit-GNs composite. Moreover, it should be mentioned that based on the XPS results, in a typical synthesis of AuNPs/Cit-GNs, AuNPs/PVP-GNs AuNPs/GNs and Cit-AuNPs, the weight ratios of Au in the products were 26.3%, 24.8%, 32.1% and 47.7%, respectively.

### The peroxidase-like activity of the AuNPs/Cit-GNs composite

To demonstrate the peroxidase-like activity of the AuNPs/Cit-GNs composite, the catalytic oxidation of the peroxidase substrate TMB in the presence of $H_2O_2$ was tested. Fig. 3A shows the photographs of the TMB solutions with different additions in 10 min. It is clear that the TMB solution in the presence of $H_2O_2$ exhibits no color change, indicating that the oxidation reaction occurs slowly in the absence of enzyme mimics. In contrast, it is interesting that the TMB + $H_2O_2$ solution changes to a blue color after the addition of enzyme mimics. It is also important to mention that with the addition of the AuNPs/Cit-GNs composite, the blue color of the solution is much deeper than the other three solutions containing the

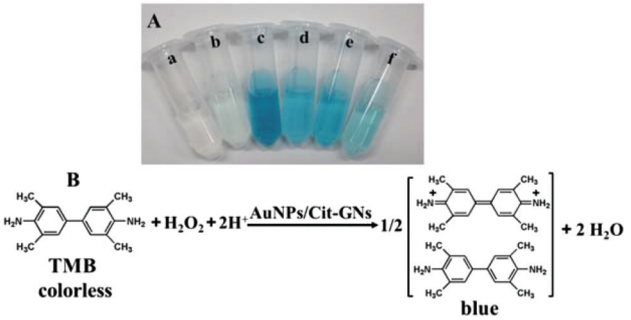


Fig. 3 (A) The color evolution of TMB in different reaction systems: (a) TMB + $H_2O_2$; (b) TMB + AuNPs/Cit-GNs; (c) TMB + $H_2O_2$ + AuNPs/Cit-GNs; (d) TMB + $H_2O_2$ + Cit-AuNPs; (e) TMB + $H_2O_2$ + AuNPs/GNs; (f) TMB + $H_2O_2$ + AuNPs/PVP-GNs. TMB: 200 μM; $H_2O_2$: 100 mM; NaAc–HAc buffer: pH = 3.8; time: 10 min. (B) The corresponding reaction scheme for the AuNPs/Cit-GNs catalysis $H_2O_2$ reduction with TMB.

same Au amount of Cit-AuNPs, AuNPs/GNs and AuNPs/PVP-GNs. Additionally, the addition of the AuNPs/Cit-GNs into the TMB solution in the absence of $H_2O_2$ fails to give a blue colored solution. These results support that AuNPs/Cit-GNs can catalyze the oxidation of TMB in the presence of $H_2O_2$ and exhibits a higher peroxidase-like catalytic ability than the other three composites. The reaction scheme is described in Fig. 3B as follows: in the presence of $H_2O_2$, TMB is catalyzed by the AuNPs/Cit-GNs which act as peroxidase, and then a blue charge-transfer complex (chromogen) is quickly formed. Therefore, the absorbance of converted TMB provides a way to monitor the catalytic reaction at 652 nm.

Similar to peroxidase, the catalytic activity of the AuNPs/Cit-GNs is dependent on the pH, temperature, and concentrations of TMB and $H_2O_2$. Our results indicated that the catalytic efficiency of the AuNPs/Cit-GNs is higher in an acid solution than in a neutral solution (Fig. 4A). Moreover, like the natural enzyme catalyzed reaction,[11,17,36] the AuNPs/Cit-GNs catalyzed

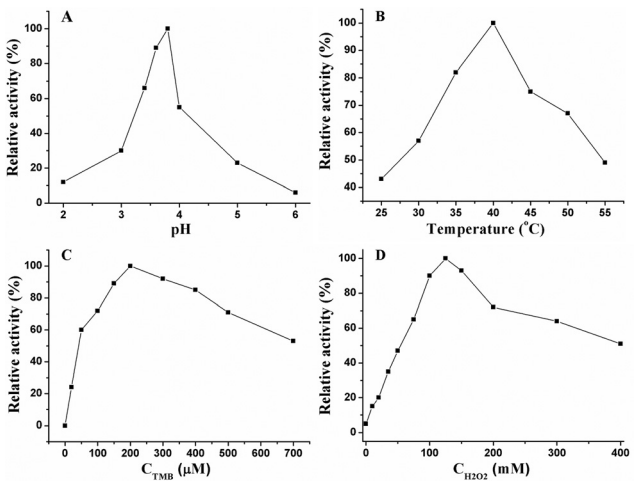


Fig. 4 The dependence of the peroxidase-like activity of the AuNPs/Cit-GNs on (A) pH, (B) temperature, (C) TMB concentration and (D) $H_2O_2$ concentration.

reaction is inhibited at high $H_2O_2$ concentrations (Fig. 4D). Based on our experiment, the maximum catalytic activity of the AuNPs/Cit-GNs was obtained under the following optimal conditions: pH 3.8, 40 °C, 200 μM TMB and 125 mM $H_2O_2$ (Fig. 4).

Previous research indicated that by simply mixing GO and Cit-AuNPs, the composite showed a good performance in the reduction of 4-nitrophenol.[37] Here, to compare the peroxidase-like catalytic ability of the direct and indirect formation of the AuNPs on GNs (or GO), we prepared the Cit-AuNPs + GO and Cit-AuNPs + GNs composites by a simply mixing method. Fig. 5A shows the UV-vis absorption spectra of the enzyme mimic catalytic reaction systems upon reaction for 10 min. The absorption peak at 652 nm suggests that TMB was oxidized. Moreover, according to these curves, the absorbances of the AuNPs/Cit-GNs are *ca.* 1.14, 1.35, 1.47, 1.76 and 2.92 times as large as those of Cit-AuNPs + GO, Cit-AuNPs + GNs, AuNPs/GNs, Cit-AuNPs and AuNPs/PVP-GNs, respectively. The inset of Fig. 5A shows the time-dependent absorbance changes at 652 nm with the addition of different kinds of enzyme mimics (the amount of Au was controlled at 0.5 μg $mL^{-1}$). In comparison with the other five composites, the absorbance at 652 nm increased quickly with the time after the addition of the AuNPs/Cit-GNs, indicating a higher catalytic activity of the composite, which is in accordance with the results of the UV-vis absorption spectra. Previous studies demonstrated that the carboxylated carbon-based materials, such as GO[11] and $C_{60}$,[12] possessed the intrinsic peroxidase-like activity because they can increase the Fermi level and the electrochemical potential from the lowest unoccupied molecular orbital (LUMO) of $H_2O_2$, which accelerates the electron transfer from these materials to $H_2O_2$. This can also be supported that in this test, Cit-AuNPs + GO showed a higher peroxidase-like catalytic ability than Cit-AuNPs + GNs. Moreover, comparing the color changes of the TMB-$H_2O_2$ solutions containing GNs and Cit-GNs, the Cit-GNs express a light blue color change, which suggested that citrate with many carboxyl groups is beneficial for the improvement of the peroxidase-like activity. However, the blue color of the solution containing AuNPs/Cit-GNs is much deeper than that of the Cit-GNs, showing that the AuNPs played an importance role in the catalytic reaction (Fig. S1†). In the case of Cit-AuNPs + GO, as the AuNPs are not

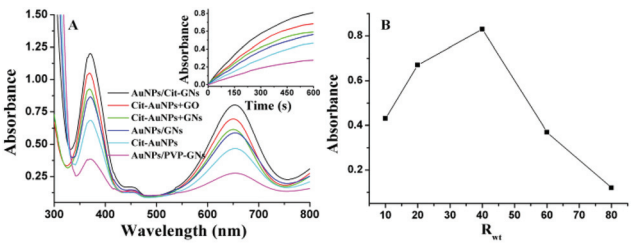


Fig. 5 (A) The UV-vis absorption spectra of various enzyme mimic catalytic reaction systems upon reaction for 10 min. The inset shows the time-dependent absorbance changes at 652 nm of the TMB reaction solutions catalyzed by these enzyme mimics. (B) The absorbance at 652 nm against different weight ratios ($R_{wt}$) of citrate to GO in the preparation of the AuNPs/Cit-GNs.

formed directly on the GO, the interaction between the AuNPs and GO is not strong enough, which affect their further enzyme mimic performance. Fig. 5B shows the absorbance at 652 nm against different weight ratios ($R_{wt}$) of citrate to GO in the preparation of AuNPs/Cit-GNs. It is clear that after the same period of time (10 min), the absorbance was increased gradually with increasing $R_{wt}$ until it reached at 40. After that, the peak decreased with the increase of the $R_{wt}$ value. As TMB contains two amino groups, a negatively charged NP surface may attract them more easily. Therefore, a suitable amount of citrate as the capping agent is beneficial for the enhancement of their peroxidase-like activity. This can be further supported by comparing the peroxidase-like activity with another substrate, ABTS. In contrast to TMB, ABTS is a negatively charged chromogenic substrate which has two sulfo groups per molecule (Scheme S1†). Therefore, the same negatively charged capping agent, citrate, on the surface of the AuNPs is unfavorable for attracting ABTS, which resulted in the lower peroxidase-like catalytic ability of the AuNPs/Cit-GNs comparing with that of the non-surfactant AuNPs/GNs (Fig. S2†). In addition, it should be mentioned that the intrinsic reduction activity of citrate has a negative effect on the peroxidase-like activity.[15] Therefore, the $R_{wt}$ of citrate to GO should be carefully controlled to duplicate the catalytic activity of the AuNPs/Cit-GNs. Based on these observations, the reason for the higher peroxidase-like activity of the AuNPs/Cit-GNs composite can be concluded as follows: (i) comparing with Cit-AuNPs, the introduced GNs can enlarge the surface area of the composite, which means more catalytic active sites will be generated on the surface of the AuNPs/Cit-GNs; (ii) a suitable amount of the negatively capping agent, citrate, with many carboxyl groups on the surface of the AuNPs is beneficial for attracting the amino groups of TMB electrostatically, which means that the affinity of the AuNPs/Cit-GNs with TMB would be much stronger than that of the AuNPs/GNs and AuNPs/PVP-GNs with TMB.

For further analysis of the catalytic mechanism and a comparison of different enzyme mimics, the apparent steady-state kinetic parameters were determined. A series of experiments were performed by changing the concentration of one substrate and keeping constant the concentration of the other. In a certain range of substrate concentrations, typical Michaelis–Menten curves can be obtained as shown in Fig. 6A and B for TMB and $H_2O_2$, respectively. The data were fitted to the Michaelis–Menten equation, in which the basic parameters can be obtained by using Lineweaver–Burk double reciprocal plots (Fig. 6C and D). For the purpose of comparison, the kinetic data, including the Michaelis constant ($K_m$) and the maximal velocity ($v_{max}$) of the enzyme mimics and previously reported HRP[36] are listed in Table 1. The $K_m$ value for the AuNPs/Cit-GNs with TMB was 0.059 mM, which is much lower than that of the AuNPs/GNs (0.38 mM), Cit-AuNPs (0.74 mM), AuNPs/PVP-GNs (2.63 mM) and HRP[36] (0.43 mM). As a low $K_m$ represents the strong affinity of the enzyme to the substrates, this result indicated that the AuNPs/Cit-GNs have a significantly higher affinity for TMB than the other enzyme mimics and even the natural enzyme HRP. On the other hand, the $K_m$ value of the AuNPs/Cit-GNs with $H_2O_2$ as the substrate was 25.08 mM, which was 1.82 and 4.94 times lower than those of Cit-AuNPs and AuNPs/PVP-GNs, respectively. These results are in agreement with the fact that a lower $H_2O_2$ concentration is required for the AuNPs/Cit-GNs than the other enzyme mimics when the maximum activity was obtained. Additionally, we measured their activity over a range of TMB and $H_2O_2$ concentrations. Fig. 6C and D show the double reciprocal plots of initial velocity *versus* one substrate concentration, which were obtained for a range of concentrations of the second substrate. The slopes of the lines are parallel, which is characteristic of a ping-pong mechanism, as was observed for HRP.[36] This indicates that, like HRP, the AuNPs/Cit-GNs bind and react with the first substrate, and then releases the first product before reacting with the second substrate.

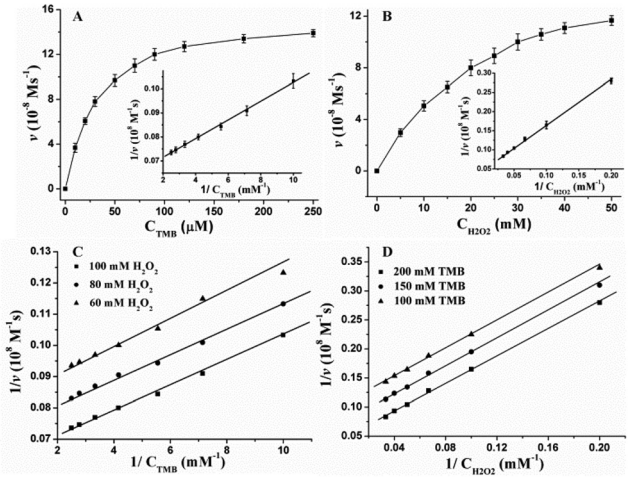


**Fig. 6** (A–B) The steady-state kinetic assay and catalytic mechanism of the AuNPs/Cit-GNs. (A) The concentration of $H_2O_2$ was 100 mM and the TMB concentration was varied. (B) The concentration of TMB was 200 μM and the $H_2O_2$ concentration was varied. The insets show the Lineweaver–Burk model for the AuNPs/Cit-GNs. (C–D) Double reciprocal plots of the activity of the AuNPs/Cit-GNs composite with the concentration of one substrate ($H_2O_2$ or TMB) fixed and the other varied. NaAc–HAc buffer: pH = 3.8; the amount of Au: 0.5 μg mL$^{-1}$.

**Table 1** A comparison of the kinetic parameters ($K_m$ and $v_{max}$) of various enzyme mimics

| | $K_m$ (mM) | | $v_{max}$ ($10^{-8}$ M s$^{-1}$) | |
|---|---|---|---|---|
| Enzyme mimics | TMB | $H_2O_2$ | TMB | $H_2O_2$ |
| AuNPs/Cit-GNs | 0.059 | 25.08 | 14.93 | 21.46 |
| AuNPs/GNs | 0.38 | 26.42 | 18.30 | 15.41 |
| Cit-AuNPs | 0.74 | 45.83 | 12.15 | 10.69 |
| AuNPs/PVP-GNs | 2.63 | 104 | 13.04 | 11.98 |
| HRP[36] | 0.43 | 3.70 | 10.00 | 8.71 |

## Conclusions

In summary, we have demonstrated that AuNPs/Cit-GNs possess intrinsic peroxidase-like activity and their catalysis is

strongly dependent on the pH, temperature and the concentration of TMB and $H_2O_2$. The kinetic analysis indicates that the catalysis is in accordance with typical Michaelis–Menten kinetics and follows a ping-pong mechanism. Moreover, due to the large surface area enhanced by the GNs, and the negative capping agent, citrate, on the surface of the AuNPs, the AuNPs/Cit-GNs reveal a higher catalytic activity to TMB than the AuNPs/GNs, Cit-AuNPs and AuNPs/PVP-GNs, and even the natural enzyme HRP. Additionally, as a mimic peroxidase, the AuNPs/Cit-GNs exhibit several advantages over natural enzymes, such as their easy preparation and preservation, low cost and stability. This work might open up possibilities for constructing Cit-GNs based materials with novel physicochemical properties in biochemistry.

## Acknowledgements

Xiaomei Chen thanks the Japan Society for the Promotion of Science (JSPS) for the fellowship. This work was financially supported by the National Natural Science Foundation of China (no. 21305050), Special Foundation for Young researchers of the Health Department of Fujian (no. 2013-2-106), the Scientific Research Foundation of Shangda Li, Jimei University (ZC2013005), and JSPS KAKENHI grant no. 2402335 and 24550100.

## Notes and references

1 J. Xie, X. Zhang, H. Wang, H. Zheng and Y. Huang, *TrAC, Trends Anal. Chem.*, 2012, **39**, 114–129.
2 G. Wulff, *Chem. Rev.*, 2002, **102**, 1–27.
3 Q. Wang, Z. Yang, X. Zhang, X. Xiao, C. K. Chang and B. Xu, *Angew. Chem., Int. Ed.*, 2007, **46**, 4285–4289.
4 R. P. Bonar-Law and J. K. M. Sanders, *J. Am. Chem. Soc.*, 1995, **117**, 259–271.
5 L. Zhu, C. Li, Z. Zhu, D. Liu, Y. Zou, C. Wang, H. Fu and C. J. Yang, *Anal. Chem.*, 2012, **84**, 8383–8390.
6 Z. Chen, L. Xu, Y. Liang and M. Zhao, *Adv. Mater.*, 2010, **22**, 1488–1492.
7 Y. P. Liu and F. Q. Yu, *Nanotechnology*, 2011, **22**, 145704.
8 J. F. Yin, H. Q. Cao and Y. X. Lu, *J. Mater. Chem.*, 2012, **22**, 527–534.
9 R. J. Cui, Z. D. Han and J. J. Zhu, *Chem.–Eur. J.*, 2011, **17**, 9377–9384.
10 W. B. Shi, Q. L. Wang, Y. J. Long, Z. L. Cheng, S. H. Chen, H. Z. Zheng and Y. M. Huang, *Chem. Commun.*, 2011, **47**, 6695–6697.
11 Y. Song, K. Qu, C. Zhao, J. Ren and X. Qu, *Adv. Mater.*, 2010, **22**, 2206–2210.
12 R. M. Li, M. M. Zhen, M. R. Guan, D. Q. Chen, G. Q. Zhang, J. C. Ge, P. Gong, C. R. Wang and C. Y. Shu, *Biosens. Bioelectron.*, 2013, **47**, 502–507.
13 Y. Jv, B. X. Li and R. Cao, *Chem. Commun.*, 2010, **46**, 8017–8019.
14 Y. F. Zhang, C. L. Xu, B. X. Li and Y. B. Li, *Biosens. Bioelectron.*, 2013, **43**, 205–210.
15 S. Wang, W. Chen, A. L. Liu, L. Hong, H. H. Deng and X. H. Lin, *ChemPhysChem*, 2012, **13**, 1199–1204.
16 H. Jiang, Z. H. Chen, H. Y. Cao and Y. M. Huang, *Analyst*, 2012, **137**, 5560–5564.
17 Z. Q. Gao, M. D. Xu, L. Hou, G. N. Chen and D. P. Tang, *Anal. Chim. Acta*, 2013, **776**, 79–86.
18 L. J. Chen, B. Sun, X. D. Wang, F. M. Qiao and S. Y. Ai, *J. Mater. Chem. B*, 2013, **1**, 2268–2274.
19 W. W. He, H. M. Jia, X. X. Li, Y. Lei, J. Li, H. X. Zhao, L. W. Mi, L. Z. Zhang and Z. Zheng, *Nanoscale*, 2012, **4**, 3501–3506.
20 C. L. Sun, X. L. Chen, J. Xu, M. J. Wei, J. J. Wang, X. G. Mi, X. H. Wang, Y. Wu and Y. Liu, *J. Mater. Chem. A*, 2013, **1**, 4699–4705.
21 Y. F. Shi, S. J. Li, Y. H. Zhou, Q. P. Zhai, M. Y. Hu, F. S. Cai, J. M. Du, J. M. Liang and X. Y. Zhu, *Nanotechnology*, 2012, **23**, 485603.
22 A. Retnakumari, S. Setua, D. Menon, P. Ravindran, H. Muhammed, T. Pradeep, S. Nair and M. Koyakutty, *Nanotechnology*, 2010, **21**, 055103.
23 M. C. Daniel and D. Astruc, *Chem. Rev.*, 2004, **104**, 293–346.
24 Y. Maeda, Y. Lizuka and M. Kohyama, *J. Am. Chem. Soc.*, 2013, **135**, 906–909.
25 A. Comin, K. Korobchevskaya, C. George, A. Diaspro and L. Manna, *Nano Lett.*, 2012, **12**, 921–926.
26 J. D. Hwang, Y. L. Lin and C. Y. Kung, *Nanotechnology*, 2013, **24**, 115709.
27 X. M. Chen, G. H. Wu, Y. Q. Jiang, Y. R. Wang and X. Chen, *Analyst*, 2011, **136**, 4631–4640.
28 X. M. Chen, G. H. Wu, J. M. Chen, X. Chen, Z. X. Xie and X. R. Wang, *J. Am. Chem. Soc.*, 2011, **133**, 3693–3695.
29 X. M. Chen, B. Y. Su, G. H. Wu, C. Y. Yang, Z. X. Zhuang, X. R. Wang and X. Chen, *J. Mater. Chem.*, 2012, **22**, 11284–11289.
30 X. M. Chen, Z. X. Cai, X. Chen and M. Oyama, *Carbon*, 2014, **66**, 387–394.
31 M. Liu, H. M. Zhao, S. Chen, H. T. Yu and X. Quan, *Chem. Commun.*, 2012, **48**, 7055–7057.
32 M. Liu, H. M. Zhao, S. Chen, H. T. Yu and X. Quan, *ACS Nano*, 2012, **6**, 3142–3151.
33 L. J. Cote, F. Kim and J. X. Huang, *J. Am. Chem. Soc.*, 2009, **131**, 1043–1049.
34 A. Ali Umar and M. Oyama, *Cryst. Growth Des.*, 2005, **5**, 599–607.
35 H. J. Yin, H. J. Tang, D. Wang, Y. Gao and Z. Y. Tang, *ACS Nano*, 2012, **6**, 8288–8297.
36 L. Z. Gao, J. Zhuang, L. Nie, J. B. Zhang, Y. Zhang, N. Gu, T. H. Wang, J. Feng, D. L. Yang, S. Perrett and X. Y. Yan, *Nat. Nanotechnol.*, 2007, **2**, 577–583.
37 F. L. Bei, X. L. Hou, S. L. Y. Chang, G. P. Simon and D. Li, *Chem.–Eur. J.*, 2011, **17**, 5958–5964.

 